CHAPTER V
RESULTS

5.1 Quality and Quantity of total-RNA

Total-RNA was isolated from the second leaf away from the shoot as described in the Methods section. The quality of the total-RNA was examined on agarose gel (1%). It was found that the total-RNA contained eukaryotic ribosomes as shown by two distinct bands of 28S and 18S rRNAs (Figure 25).

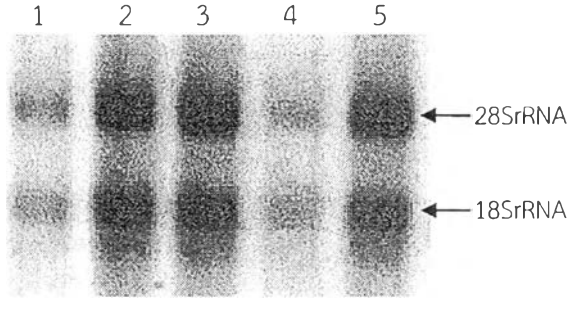

Figure 25 Quality evaluation of the isolated total-RNA preparation. Two distinct bands of 28S and 18S rRNAs on 1% agarose gel. Lanes 1-5 is a total-RNA.

The concentration and purity of the total-RNA preparation were determined spectrophotomecally at 260 nm to obtain the UV absorbance value of nucleic acid. The ratio of absorptions at 260 nm vs 280 nm is commonly used to assess DNA contamination of protein solutions, since proteins (in particular, the aromatic amino acids) absorb light at 280 nm. The absorbance at 230 nm is reliable for quantitative determination of protein stability, from the absorbance values, the concentrations of various total-RNA preparations were then calculated, and the results are shown in Table 21. It can be seen that the concentrations of the total-RNA were obtained in a range from 128 to 280 ng/µl.

In terms of purity, the total-RNA was determined as the value of A260/A280 ratio. In general, the values in the range from 1.8 to 2.0 indicate that the total RNA is relatively pure. The values lower than the range mean the total-RNA might be contaminated with phenols, proteins or others which also absorb light at the same wavelength of 280 nm. The results showed that the A260/A280 values of the 5 total-RNA preparations were in the range from 1.48 to 1.72 (Table 21), suggesting that

our method of preparation was fairly good, with relatively low amount of contaminations. Another value of A260/230 which means the contamination of the polysaccharides found in plant was also evaluated. In general, the ratio is expected to be the same as the ratio of A260/280. Our results showed that the A260/230 ratios of the total-RNA were in the range from 0.33 to 0.63 (Table 21), suggesting that RNA isolation were not pure.

Table 21 Concentration and purity of total-RNA based on spectrophotometer method.

RNA (2 µl)	ng.µl^{-1}	A260	A280	A260/280	A260/230
RNA_1	202.1	5.052	3.156	1.60	0.47
RNA_2	136.2	3.406	1.983	1.72	0.39
RNA_3	282.1	7.052	4.778	1.48	0.67
RNA_4	128.1	3.201	2.126	1.51	0,33
RNA_5	155.0	3.975	2.345	1.65	0.44

5.2 Quality and Quantity of cDNA

The quality of the cDNA was determined by the PCR-based method using the 18S rRNA as primer pairs as listed in Table 22. The PCR-products was found to have a thick band of 536 bp on the 1% agarose gel (Figure 26), indicating that mRNA could be transcribed to cDNA.

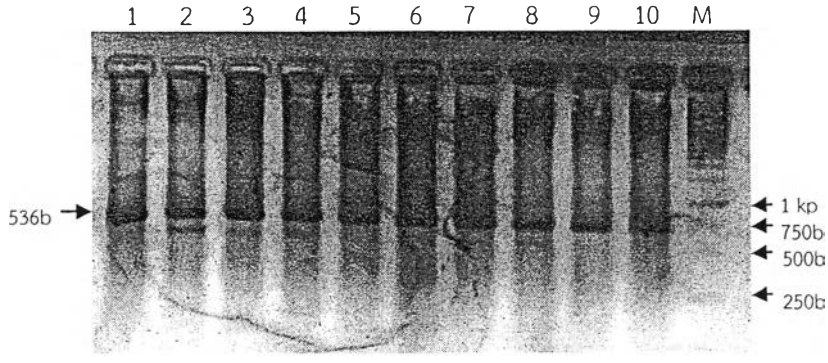

Figure 26 Quality of the cDNA. The PCR-product which was amplified from the 18S rRNA primer pairs, and run on 1%agarose gel.

Similar to the RNA determination, the cDNA concentration was also measured by nucleic acid absorbtion at 260 nm. It was found that the cDNA concentrations were in the range from 900 to 1,500 ng/µl (Table 22). For its purity based on protein contamination (A260/A280) and polysaccharide contamination (A260/A230), it was found that to be in the good narrow average ratios of 1.7 and 2.2, respectively (Table 22). Therefore, the quality and quantity of the obtained cDNA preparations were also acceptable and were used for subsequent studies.

Table 22 Concentration and purity of cDNA based on spectrophotometer method.

DNA (2 µl)	ng.µl^{-1}	A260	A280	A260/280	A260/230
1	1464.5	29.29	16.27	1.80	2.27
2	1345	28.89	15.07	1.78	2.25
3	1280.8	25.62	14.28	1.79	2.30
4	1109.9	22.199	12.599	1.76	2.14
5	1031.4	20.628	11.826	1.74	2.11
6	1063.5	21.271	12.148	1.75	2.16
7	907.6	18.151	10.388	1.75	2.12
8	1088	21.760	12.424	1.75	2.11
9	141.1	22.834	13.005	1.76	2.13
10	1111.6	22.231	12.649	1.76	2.14

5.3 Gene fragment amplification

PCR-products of each step were cloned into the pGEM-T easy vector, followed by the steps of plasmid preparation, restriction enzyme digestion, gel electrophoresis, and sequencing to confirm the correct insertion before going to the next step (Figure 27).

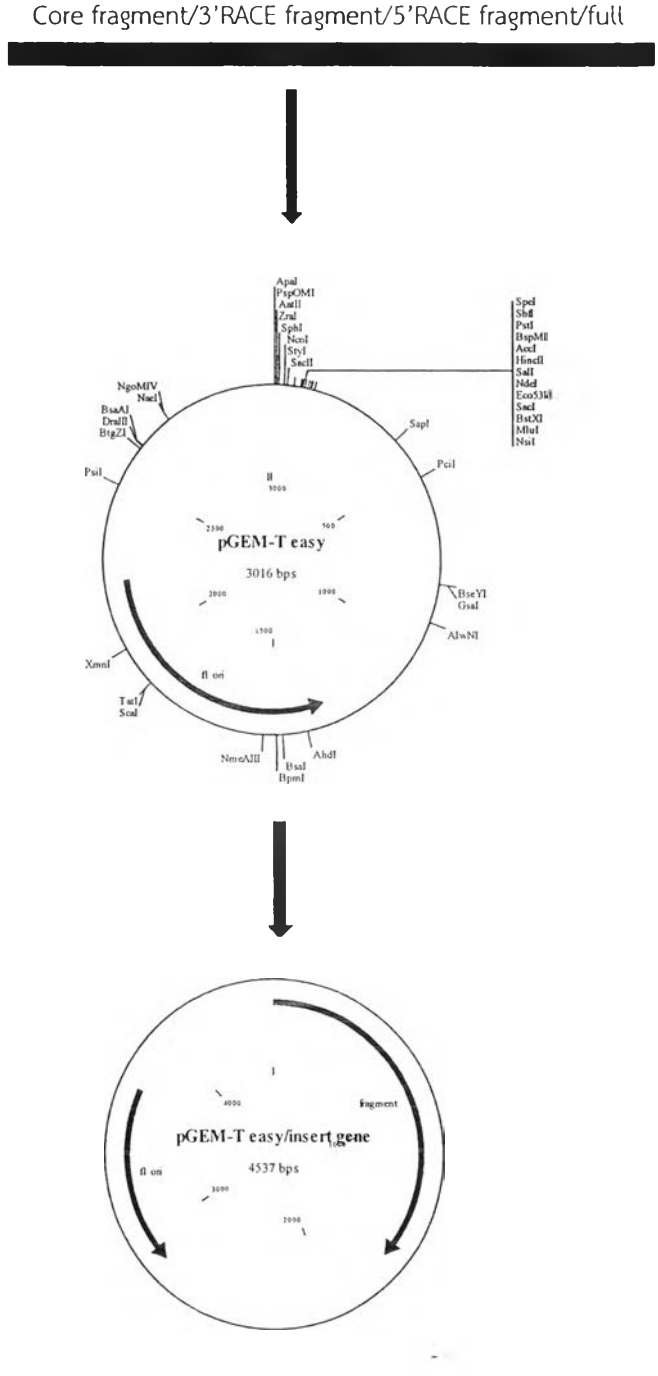

Figure 27 Steps of gene cloning into pGEM-T easy vector.

5.3.1 Core fragment amplification using degenerated primers

Core fragments of *CsCPR*, *CsG10H*, and *CsGG18H* were amplified by using the generated primer pairs as listed in Table 6. The PCR-products run on 1% agarose appeared to have the expected sizes of 1613 bp and 975 bp, respectively (Figure 28).

5.3.2 3′RACE and 5′RACE fragments

The 3′RACE and 5′RACE fragments of *CsCPR*, CsG10H, and CsGG18H were amplified using their specific primers and the primers provided with the kit as listed in Table 7 As show in Figure 28, the PCR-products for the 3′RACE of *CsCPR*, *CsG10H*, and *CsGG18H* were obtained with the expected sizes on 1% agarose gel of 685 bp, 529 bp, and 652 bp, respectively. The PCR-products for the 5′RACE of the three genes were obtained with the expected sizes on 1% agarose gel of 529 bp, 458 bp, and 470 bp, respectively.

The three fragments (core fragments, 5′-RACE and 3′-RACE fragments) of the three genes were then analyzed for their consensus sequences by assembly the fragments using the program CloneManager 9.1. The obtained fragments were then used as template to design for full-length primer pairs.

5.3.3 Full-length fragments

The full-length genes of *CsCPR*, *CsG10H*, and *CsGG18H* could be found from their start codon to stop codons and predicted the open reading frames (ORFs) using the same CloneManager 9.1 program. The ORFs of *CsCPR*, *CsG10H*, and *CsGG18H* were found to be 2300, 1521, and 1413 bp, respectively (Figure 28).

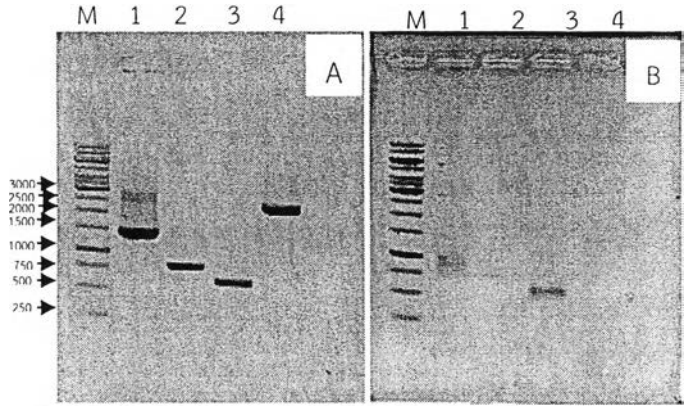

Figure 28 PCR-products of fragment amplification. (A) Fragment of *CsCPR* and (B) fragment of *CsGG18H*. The PCR-product was run on 1% agarose gel represented the core fragment (lane 1), 3′-RACE PCR fragment (lane 2), 5′-RACE PCR fragment (lane 3), and full-length fragment (lane 4).

5.4 Cloning

Every fragment of PCR product were cloned into propagate vector, pGEM-T easy vector (Figure 30), for general cloning to confirmed and checked for the insertion.

The serial PCR amplification from core fragment to 3′-, 5′- RACE fragment and full length fragment were cloned and confirmed by *EcoRI* enzymatic restriction reaction before plasmid purified as described in Section 4.13 and sequencing confirmed. For pGEM-T easy vector (3 kb) separated containing the insert CsGG18H (1.4 kb), and CsCPR (2.3 kb) were digested and fragment separated using agarose gel (Figure 29).

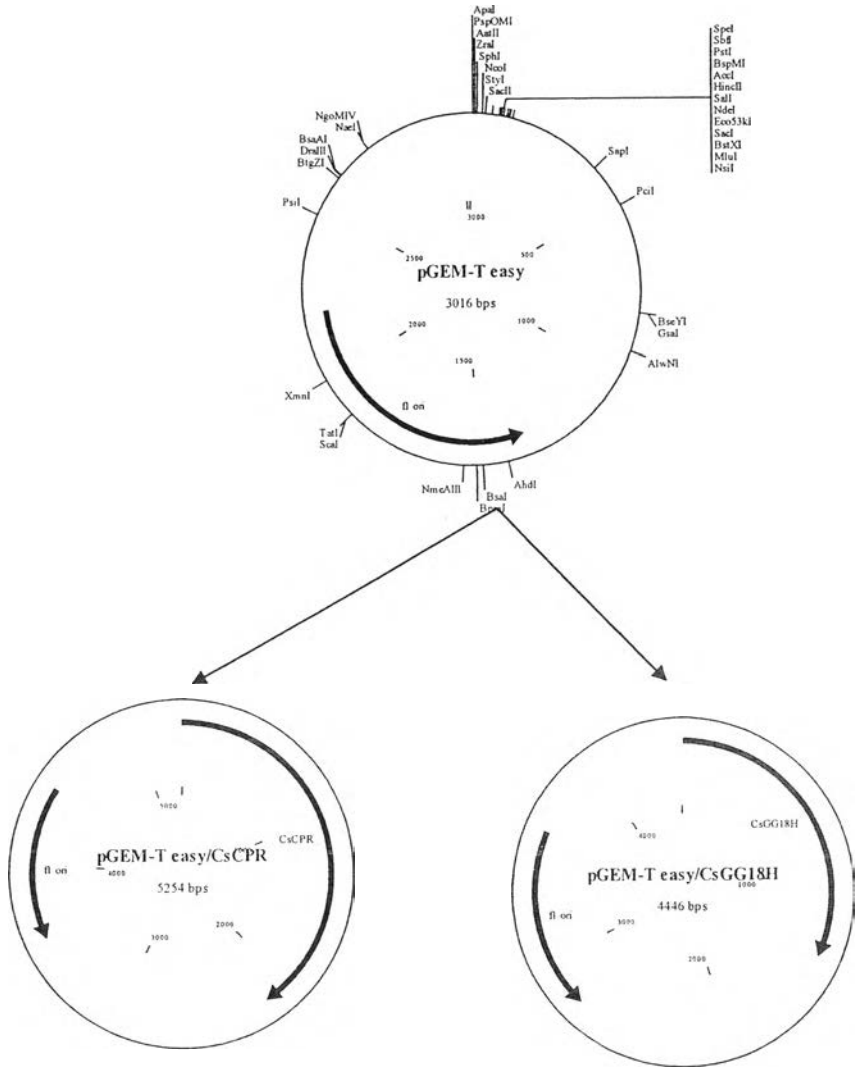

Figure 29 Flow chart of the inserted gene in pGEM-T easy vector.

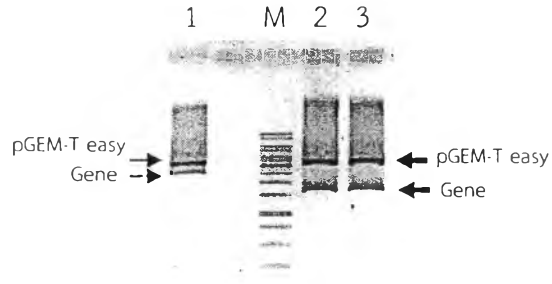

Figure 30 Recombinant genes in pGEM-T easy vector using *EcoR*I restriction enzyme digestion checked for insertion. Lane 1: CsCPR recombinant, lane 2: CsG10H recombinant, lane 3: CsGG18H recombinant, lane M: 1 kb DNA ladder.

5.5 Sequence analysis

Sequences and chromatograms derived from sequencing were analyzed in CloneManager9.0 program by trim off the plasmid and primer. Sequences were then submitted to the NCBI database as accession number KF738254 and KF738256 for *CsCPR* and *CsGG18H*. By personal communication, CsGG18H were identified and named as CYP97C27 based on the nomenclature system established by David Nelson's committee group (http://drnelson.utmem.edu/CytochromeP450.html) (Nelson, 2006). The good quality sequence was further:

5.5.1 Biology of Sequences

Sequence was translated in frame (6-frame translation) using CloneManager 9.0 into putative amino acid. For CsCPR and CsGG18H putative protein were 711 and 471 amino acid residues, respectively. All two putative proteins were predicted the function domain group by blastx algorithm and shown the significant E values from PSI- and PHI-blast searches against the conserved domain database (CDD) at NCBI. Sequences were then predicted for the monomeric molecular weight using http://web.expasy.org/compute_pi/ and they were 78744.45 and 52834 Da with the theoretical pI were 5.27 and 5.93 of CsCPR and CsGG18H, respectively (Table 23).

Table 23 Sequence analysis data

Putative protein	ORF (bp)	Amino acid (residues)	pI	MW (kDa)
CsGG18H	1413	471	5.94	52.83
CsCPR	2300	711	5.27	78.74

5.5.2 Sequence characterization

5.5.2.1 Cytochrome P450

The cytochrome P450, CsGG18H, deduced protein sequence were multiple alignments using the GeneDoc program (Nicholas et al., 1997) and found the cytochrome P450 characteristic domains including the oxygen binding and heme-binding in both cytochrome P450 families (Figure 31).

1. Heme-binding domain FXXGXRXCXG, the amino acid residues were corresponding to Phe400-Ser-Gly-Gly-Pro-Arg-Lys-Cys-Val-Gly409

2. Oxygen binding domain (A/G)GX(D/E)T(T/S) were corresponding to Ala267-Gly-His-Glu-Thr-Thr272

3. The P450 could be found the cluster of ERR triad, Glu-Arg-Phe.

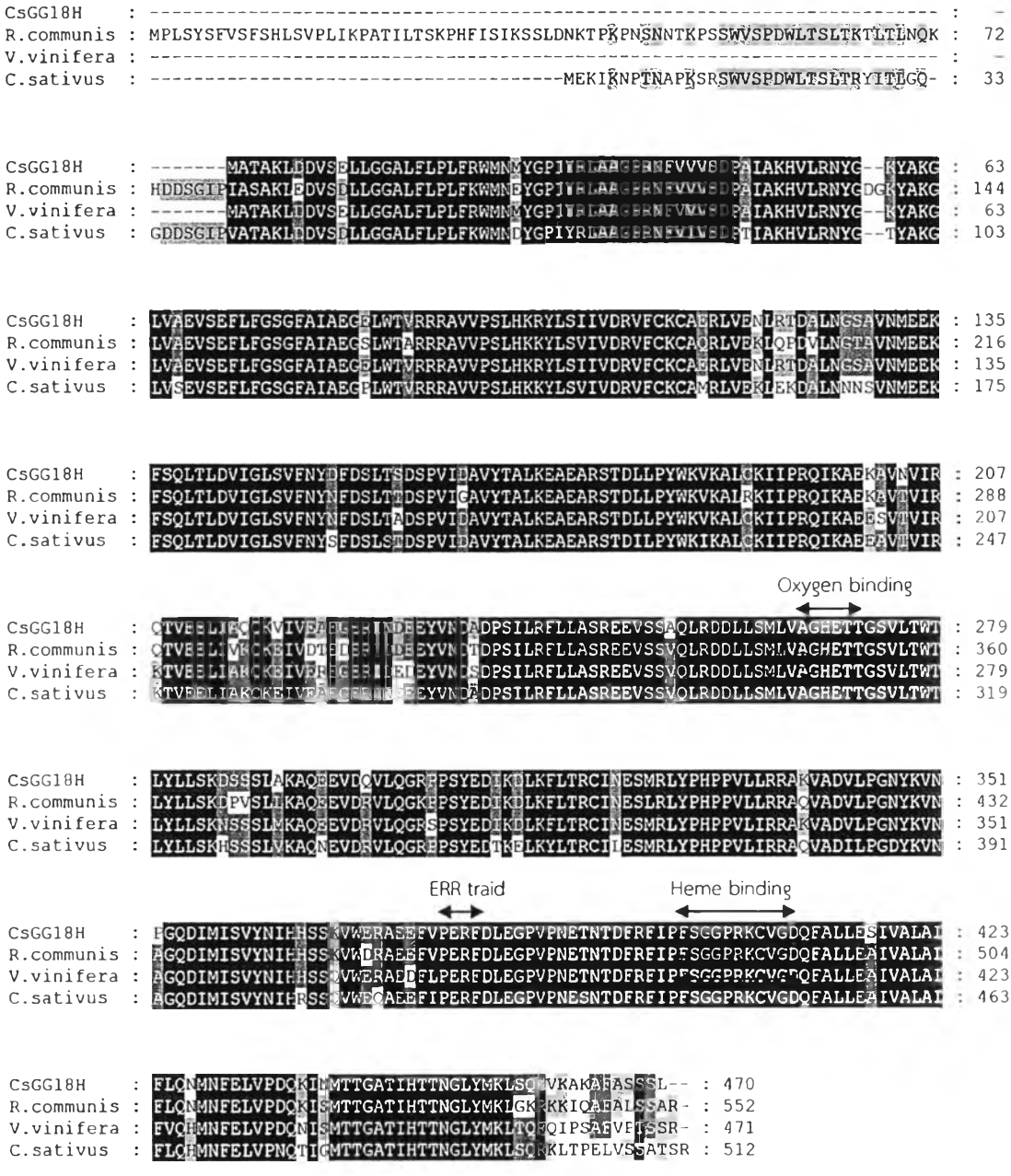

Figure 31 Amino acid alignment of CYP97 family. The alignment was done based on homologous amino acid sequences retrieved from other plant host from blastx (nucleotide translated blast) in NCBI database using GeneDoc program (Nicholas et al., 1997). The protein shown in the alignment are from *Ricinus communis* (R.communis, GenBank ID: XP002519427); *Vitis vinifera* (V.vinifera, GenBank ID: CBI30186); CsCYP97, *Croton stellatopilosus* (GenBank ID: KF738256); *Cucumis sativus* (C.sativus, GenBank ID: XP004156328). The arrow lines indicate a cluster of, a heme binding domain (FXXGXRXCXG) and an oxygen binding domain (A/G)GX(D/E)T(T/S). Identical amino acid residues are boxed in black and similar residues are shaded in gray. Gaps are inserted to maximize homology.

5.5.2.2 Cytochrome P450 reductase

The CsCPR characteristic domains were indicated in the Figure 32 composed of two binding site of FMN, FAD, NADPH and one binding domain of P450 are corresponded in amino acid sequences below;

1. FMN binding domain; Thr91-Val-Thr-Ile-Tyr-Gly-Thr-Gln-Thr-Gly-Thr-Ala-Glu-Gly-Phe-Ala-Lys-Ala-Phe-Ala-Glu-Glu112 and Ala165-Thr-Gly-Asp-Gly-Glu-Pro-Thr-Asp-Agn-Ala-Ala-Arg-Phe-Tyr-Glu-Gly-Lys-AspArg-Gly-Glu-Trp-Leu-Arg-Asn-Leu-Lys-Phe-Gly-Val-Gln-Tyr-Glu-His-Phe-Asn-Lys-Leu-Asp-Glu206

2. FAD binding domain; Glu320-Leu-His-Thr-Pro-Ala-Ser-Asp-Cys-Thr-His-Leu-Gly-Phe-Asp-Ile-AlaGly-Thr-Gly-Leu-Tyr-Glu-Thr-Gly-Asp-His-Val-Gly-Val-Tyr-Cys-Glu-Asn263 and Ala483-Pro-Arg-Leu-Gln-Pro-Arg-Tyr-Tyr-Ser-Ile-Ser-Ser-Ser-Pro-Ser-Met-Ala-Pho-Ser-Arg-Ile-His-Val-Yhr-Cys-Ala-Leu-Val511

3. NADPH binding domain; Gly220-Leu-Gly-Asp-Asp-Asp-Glu-Cys-Ile-Gle-Asp-Asp-Phe-Thr-Ala-Trp235 and Pho562-Ile-Ile-MetIle-GlyPro-Gly-Thr-Gly-Leu-Ala-Pro-Phe-Arg-Gly-Phe-Leu-Gln-Glu-Arg-Leu-Ala-Gln-Leu-Gly587

4. P450 binding domain; Gly648-Ala-Tyr-Val-Tyr-Val-Cys-Gly-Asp-Ala-Lys-Gly-Met-Ala-Arg-Asp-Val-His-Lys-Ala677.

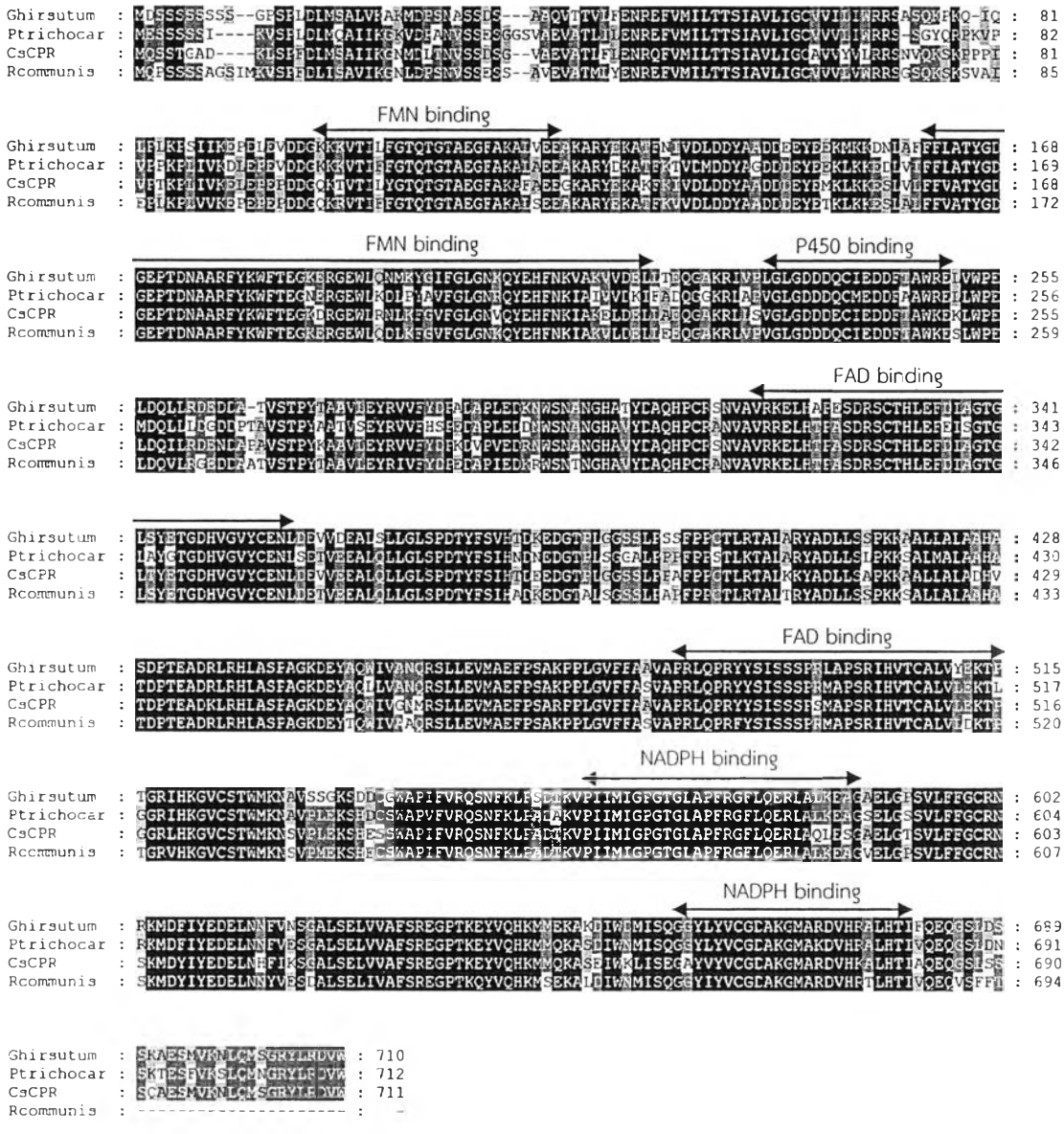

Figure 32 Amino acid alignment of CPR. The alignment was done based on homolog amino acid sequences retrieved from other plant host from blastx (nucleotide translated blast) in NCBI database using GeneDoc program (Nicholas et al., 1997). The protein shown in the alignment are from *Gossypium hirsutum* (Ghirsutum, GenBank ID: ACN54324); *Populus trichocarpa* (Ptrichocar, GenBank ID: AF302497); *Croton stellatopilosus* (CsCPR, GenBank ID: KF738254); *Ricinus communis* (Rcommunis, GenBank ID: XP002534464). The arrow lines indicate the typical motifs of P450-, NADPH-, FMN-, and FAD binding domain. Identical amino acid residues are boxed in black and similar residues are shaded in gray. Gaps are inserted to maximize homology.

5.5.2.3 Location prediction

Three amino acid sequences were predicted which kind of N-terminal sorting signals using TargetP 1.1 (http://www.cbs.dtu.dk/services/TargetP/) (Emanuelsson et al., 2007). TargetP reported a prediction score with no assigned localization for chloroplast (C)/mitochondrial (M) with the very reliable prediction (RC<4) (Table 24). Prediction of localization, based on the scores above; the possible values were that CsG10H was a secretory pathway, i.e. the sequence contains SP, CsGG18H and CsCPR were any other location (Table 24).

Table 24 TargetP v1.1 prediction results using plant network.

Name	Length	cTP	mTP	SP	Other	Location	RC
CsGG18H	471	0.007	0.263	0.215	0.582	-	4
CsCPR	711	0.220	0.034	0.063	0.714	-	3

The amino acid sequences were then submitted to SignalP 1.1 finding the signal peptide position (http://www.cbs.dtu.dk/services/SignalP/) (Figure 34). Only the G10H amino acid sequence which show the signal peptide with 0.5 score (98% of the reliable prediction).

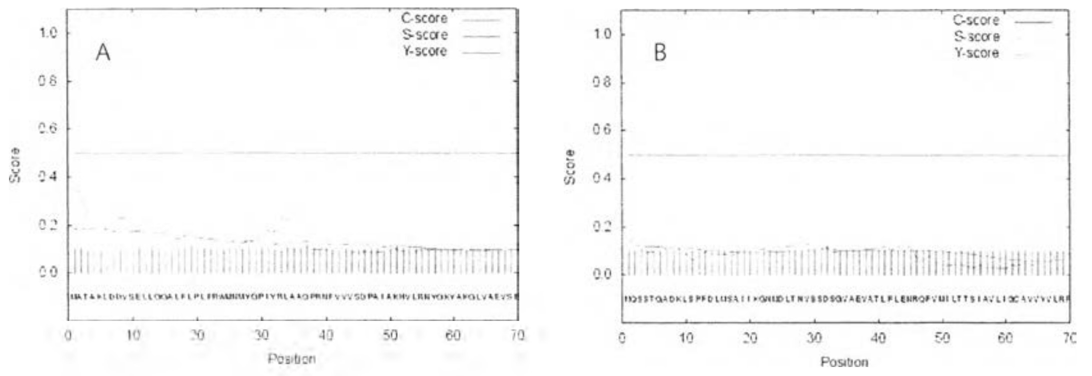

Figure 33 The graphical output of SignalP-NN, showing C-, S- and Y-score. The cleavage site is predicted to be at the position of maximal Y-score. (A) for CsGG18H and (B) for CsCPR

To check whether protein were an integral membrane proteins, try a trans-membrane α-helix predictor, TMHMM 2.0 (http://www.cbs.dtu.dk/services/TMHMM/). The amino acid sequence of CsCPR were found one trans-membrane at the N-terminal, however no found any in CsGG18H sequence (Figure 34).

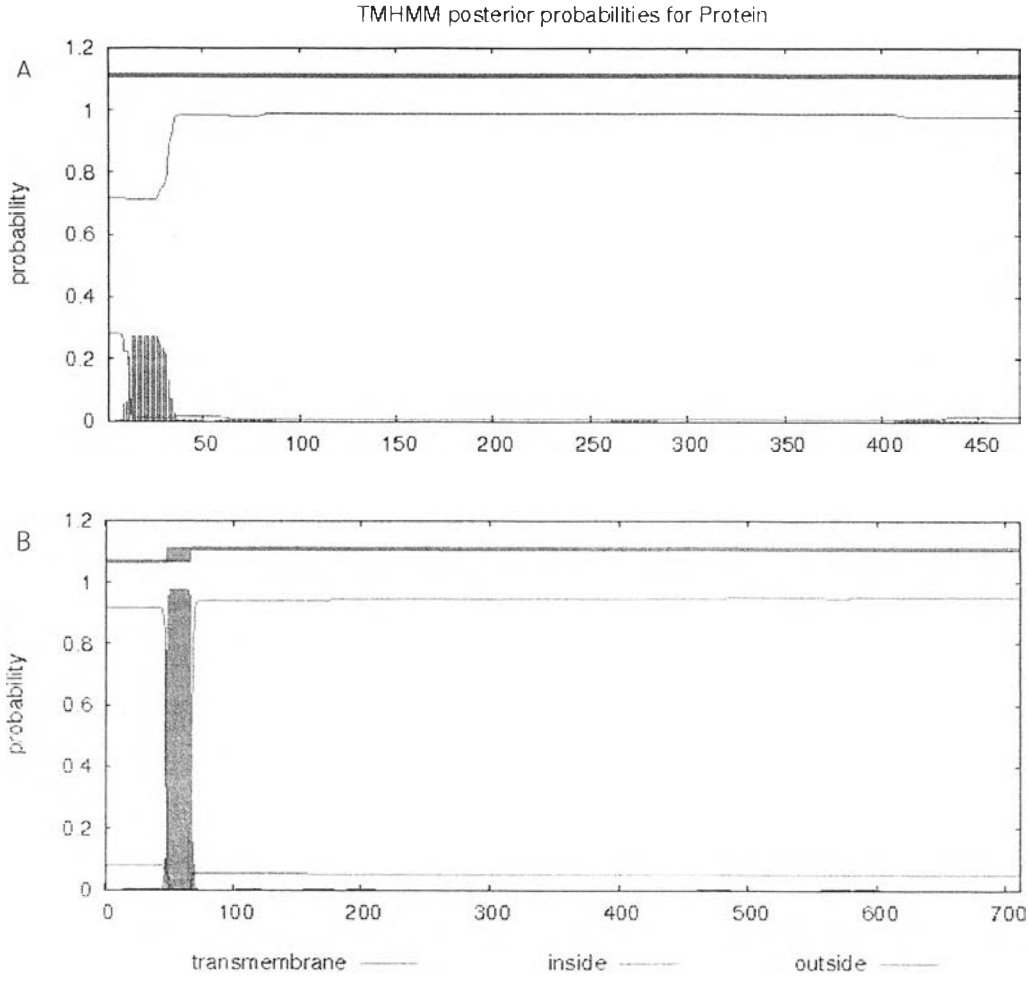

Figure 34 The graphical output of TMHMM, showing the posterior probabilities for trans-membrane, inside (i.e., cytoplasmic), and outside (i.e., luminal or exterior) regions. (A) CsGG18H and (B) CsCPR.

5.6 Phylogenetic relationship

Three phylogenetic trees of *CsGG18H* and *CsCPR* from *C. stellatopilosus* were inferred using the evolution Neighbor-Joining (NJ) method (Figure 35, 36).

5.6.1 Homology

Amino acid sequences of the three gene products were homology search using blastx algorithm in NCBI database:

CsGG18H showed high homology to *V. vinifera* (93% identity), *R. communis* (90% identity) and *Cucumis sativus* (85% identity).

The homology sequences were retrieved with the NCBI accession number to construct phylogenetic tree. It appeared that the enzymes in the CYP76 family have been reported to catalyze geraniol to form 10-hydroxygeraniol, whereas the enzymes in the CYP97 family have been reported to catalyze in the carotenoid pathway.

CsCPR, the homology of the amino acid alignment of CsCPR showed 83% identity with *R. communis* cytochrome, 81% identity with *Gossypium hirsutum*, and 79% identity with *P. trichocarpa*.

5.6.2 CYP97 family

The midpoint-rooted tree of the CPY97 family (Figure 35) showed that CsGG18H was separated in the carotenoid epsilon-ring hydroxylase group closely related with *V. vinifera*. The CPY97 of *V. vinifera* had not identified for the exact chemical reaction. The relative node was shown 99% bootstrap support.

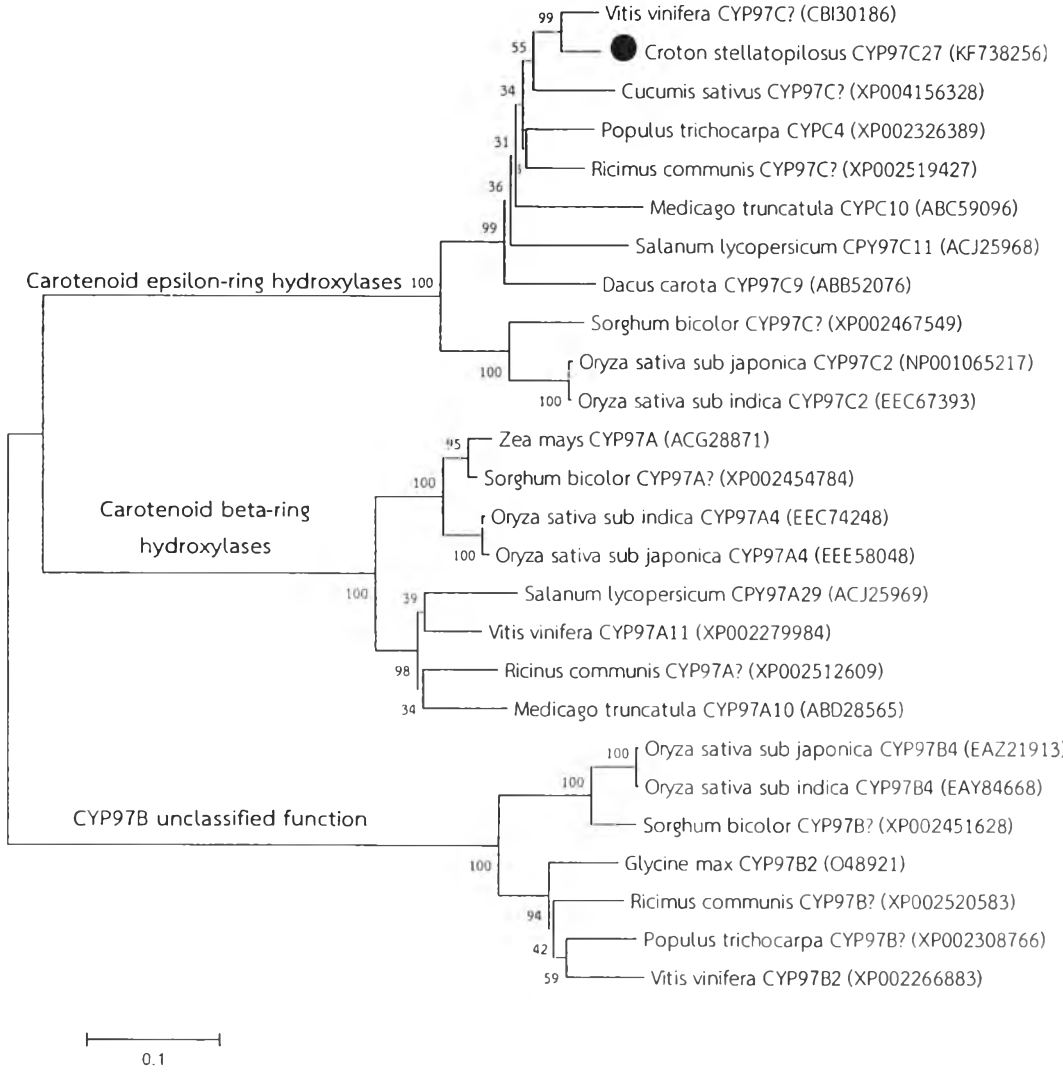

Figure 35 A midpoint-rooted Neighbor-Joining tree of CPY97 family based on the deduced amino acid sequences. The evolutionary history was inferred using the Neighbor-Joining method (Saitou and Nei, 1987). The optimal tree with the sum of branch length = 2.52024252 is shown. The percentage of replicate trees in which the associated taxa clustered together in the bootstrap test (1000 replicates) are shown next to the branches (Felsenstein, 1985). The tree is drawn to scale, with branch lengths in the same units as those of the evolutionary distances used to infer the phylogenetic tree. The evolutionary distances were computed using the JTT matrix-based method (Jones et al., 1992) and are in the units of the number of amino acid substitutions per site. The analysis involved 26 amino acid sequences. All positions containing gaps and missing data were eliminated. There were a total of 450 positions in the final dataset. Evolutionary analyses were conducted in MEGA6 (Tamura et al., 2013).

5.6.3 CPR

The CPR midpoint-rooted tree was separated into two-groups, CPR class-one and CPR class-two. The groups could be divided according to the deduced amino acid sequence with have paralogs and varies within the plant host taxa. The isoform (homolog) of the CPR depended on species which most vascular plants are shown 1 to 3 isoform such as three isoform in *P. tricacarpa* and *A. thaliana*, two isoforms in *V. vinifera*, and some reported 1 isoform in *R. communis* (Figure 36).

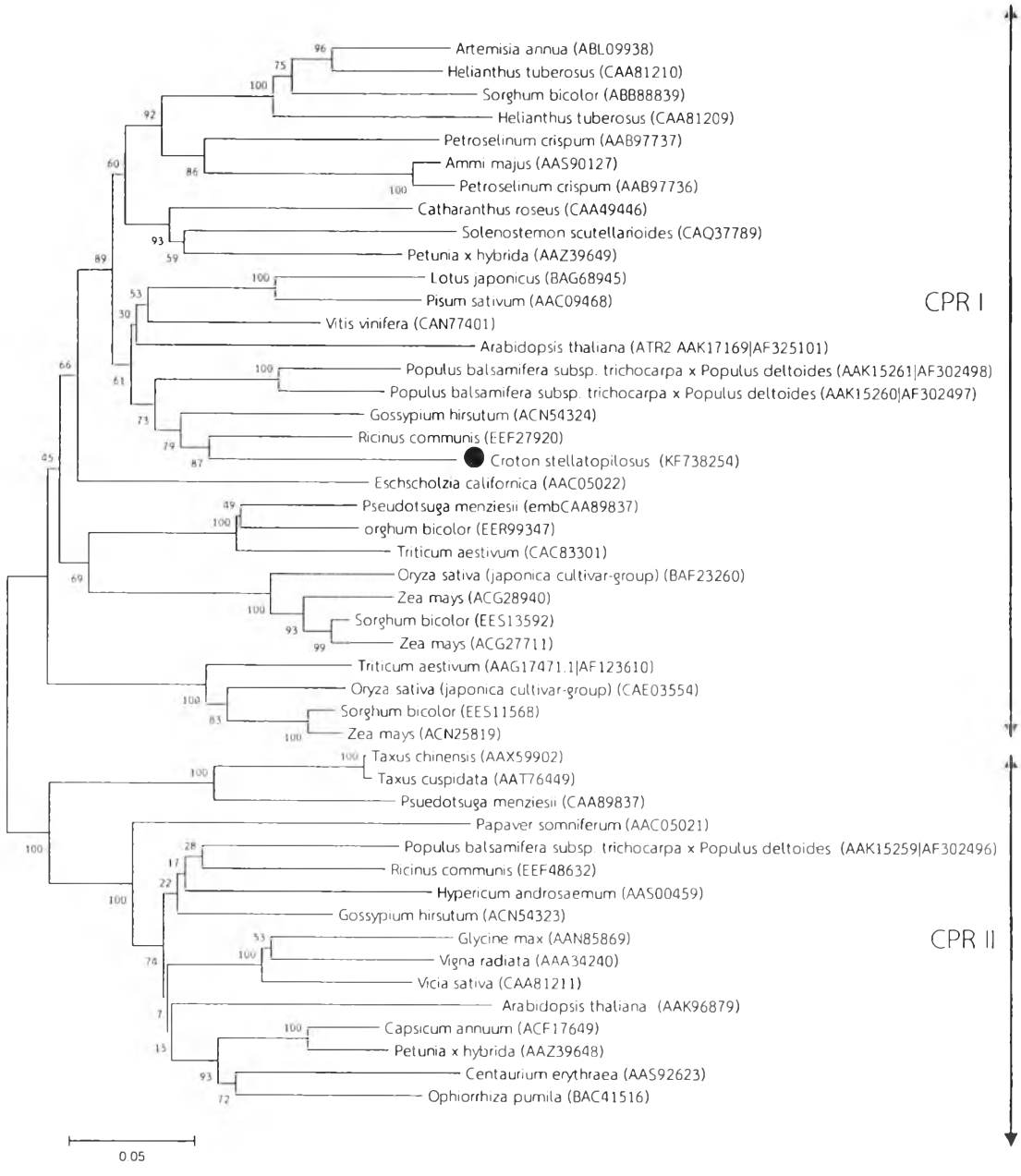

Figure 36 A midpoint-rooted Neighbor-Joining tree of cytochrome P450 reductase (CPR) family based on the deduced amino acid sequences. The evolutionary history was inferred using the Neighbor-Joining method (Saitou and Nei, 1987). The optimal tree with the sum of branch length = 3.92147280 is shown. The percentage of replicate trees in which the associated taxa clustered together in the bootstrap test (1000 replicates) are shown next to the branches (Felsenstein, 1985). The tree is drawn to scale, with branch lengths in the same units as those of the evolutionary distances used to infer the phylogenetic tree. The evolutionary distances were computed using the JTT matrix-based method (Jones et al., 1992) and are in the units of the number of amino acid substitutions per site. The analysis involved 47 amino acid sequences. All positions containing gaps and missing data were eliminated. There were a total of 541 positions in the final dataset. Evolutionary analyses were conducted in MEGA6 (Tamura et al., 2013).

5.7 Protein expression

The ORF genes were amplified with the primers flanking the compatible enzyme at the 5′-end and transformed into the cloning vector (pGEM-T easy, Promega) as described in Section 4.10 (general cloning). The obtained recombinants were confirmed by *EcoRI* restriction digestion and sequencing. The corrected recombinants were further cloned and transformed in the expression vector, pET32a (Novagen). Both of the recombinant and pET32a were compatible to enzyme digestion according to each gene (Figure 39). The inserted genes and pET32a, expression vector, were excised from the gel and purified using the method in Section 4.13.2.

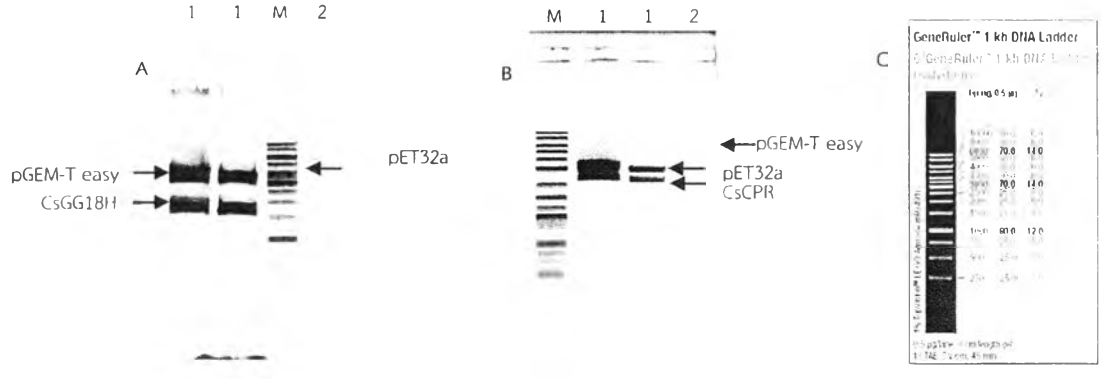

Figure 37 Restriction enzyme digestion. (A) The compatible *NotI*/*XhoI* restriction enzyme of CsGG18H and pET32a (B) The compatible *BamHI*/*SalI* restriction enzyme of CsCPR and pET32a and (C) The GeneRuler 1 kb DNA Ladder 250 to 10,000 bp (Thermo Science). Lane 1: restriction enzyme digestion indicated the pGEM-T easy vector and the inserted gene, lane 2: pET32a after restriction enzyme digestion and lane M show the marker of the GeneRuler 1 kb DNA laddar.

The fragment was freshly purified from gel and ligated into pET32a (Figure 38) and transformed into BL21(DE3) bacterial strain cell.

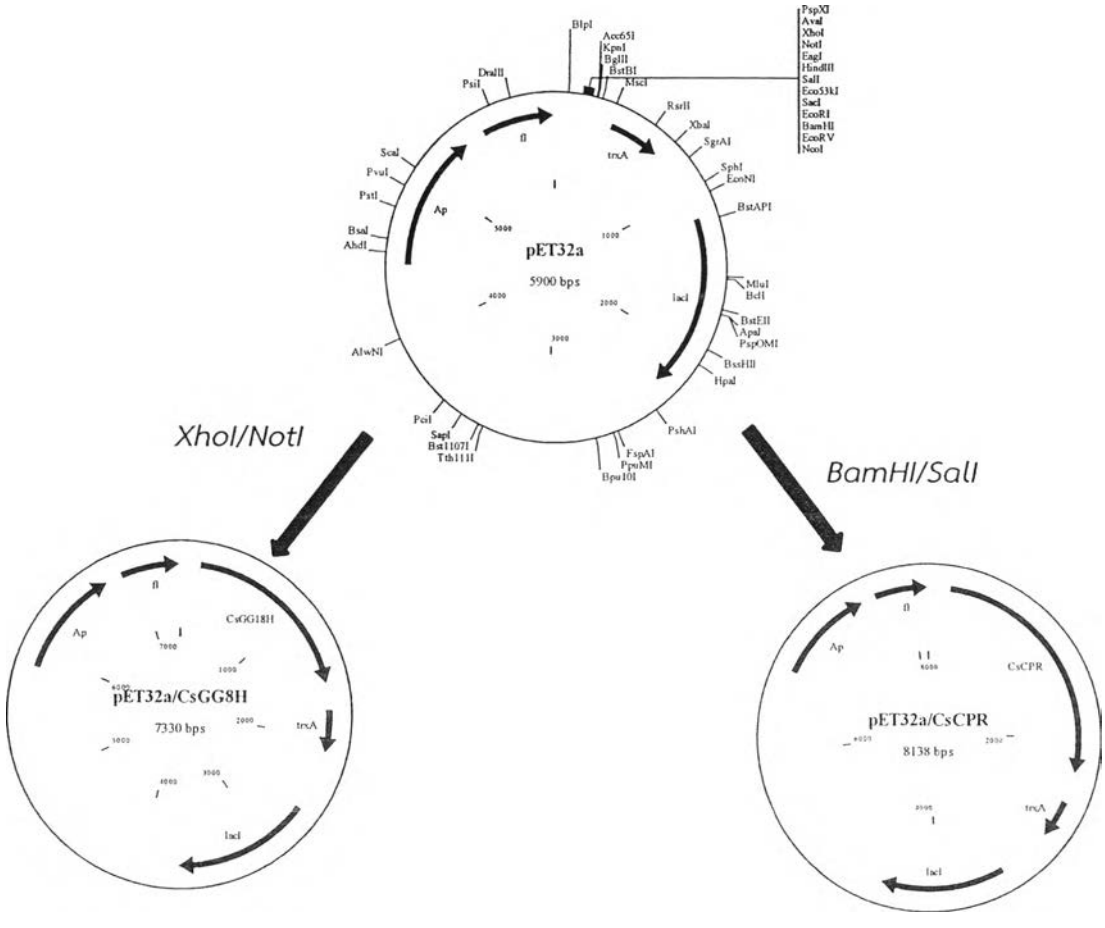

Figure 38 Flow chart of recombinant gene expressed vector. Inserted gene was ligated and cloned into pET32a expression vector at multiple cloning sites. Plasmids were drawn in CloneManaer 9.1 program.

5.8 SDS-PAGE and Western blot analysis

5.8.1 Time-course for expression

The recombinant plasmids were expressed by IPTG induction. The time course of gene expression was first tried by collecting the crude cells for 1 ml at hour 0, 2, 4, 6, 12, and 24 after IPTG induction. It was found that two genes, CsG10H, and CsGG18H could be expressed for one hour after the IPTG induction at 37°C with 220 rpm shaking. However, the CsCYP the expression seem presented on the gel after the induction of the IPTG at the overnight cells (Figure 39).

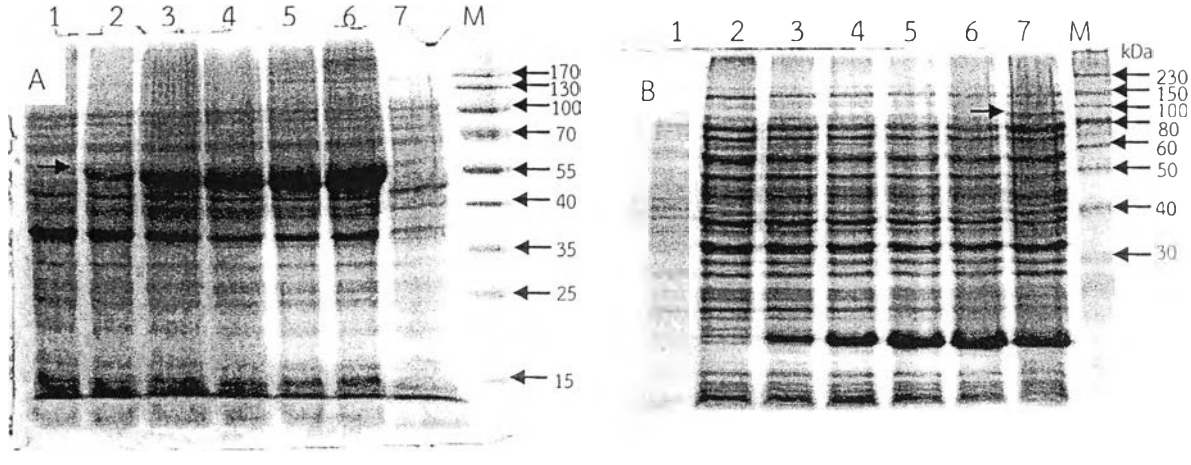

Figure 39 SDS-PAGE of the recombinant protein. (A) CsG10H, (B) CsGG18H and (C) CsCPR represented the time course induction of IPTG at lane 1 at hour0, lane 2 at hour1, lane3 at hour2, lane4 at hour4, lane5 at hour6, lane 6 at hour 24, lane 7 pET32a without inserted gene, and lane M protein ladder.

The optimal condition of the expression of the proteins;

CsGG18H, the expression protein was induced with 1 mM IPTG and 0.005 μM to induced heme and incubated at 37°C until OD_{600} reach to 0.6 with 250 rpm shaking. The culture then incubated at 4°C for 8 hr and incubated at 37°C with 250 rpm shaking for ODC with 250 rpm shaking for OD_{600} reach to 1. Cell pellet of the culture turn red mean for the heme motif had activity.

CsCPR, the optimal condition was cell induced with 1 mM IPTG after the pre-culture had OD600 equal to 0.6 and incubated the culture with 200 rpm shaking at 30°C for 40 hr.

5.8.2 Western blot

The three genes CsGG18H and CsCPR were expressed as recombinant proteins which were combined with 6 histidine (6His) amino acid residues at the C-terminal or N-terminal, for subsequent Ni-bead affinity purification (Table 25). All the three recombinant proteins could be confirmed to be present by blotting using the Alkaline Phosphatased (AP)-conjugated antibody (Invitrogen).

Table 25 Molecular weight of protein presented on the 12% acrylamide gel

Protein	6His-terminal	MW of protein (kDa)	MW of 6His (kDa)
CsCYP97	C-terminal	52.83	7
CsCPR	N-terminal	78.74	18

Proteins with the 6-Histidine tag could be stained in purple-blue on the PVDF membrane (Figure 40).

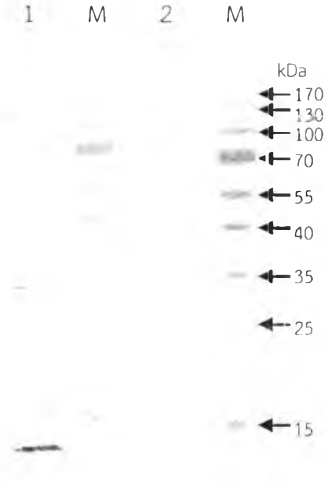

Figure 40 Western blot of three recombinant proteins. Lane 1 CsCPR, Lane 2 CsGG18H and lane M protein marker.

5.8.3 Inclusion body protein

Protein solubilization by using a detergent buffer was tried but could not solubilize by any of the lysis buffers as listed in Table 25 in Section 4.19.2. The protein was still associated with the membrane in the pellet fraction in Figure 41.

For the CsGG18H protein, all of the four lysis buffers could not solubilize the protein. Lysis buffer V and lysis buffer VI could a bit solubilize the protein as shown by the CsGG18H expected protein band on the acrylamind gel (Figure 41).

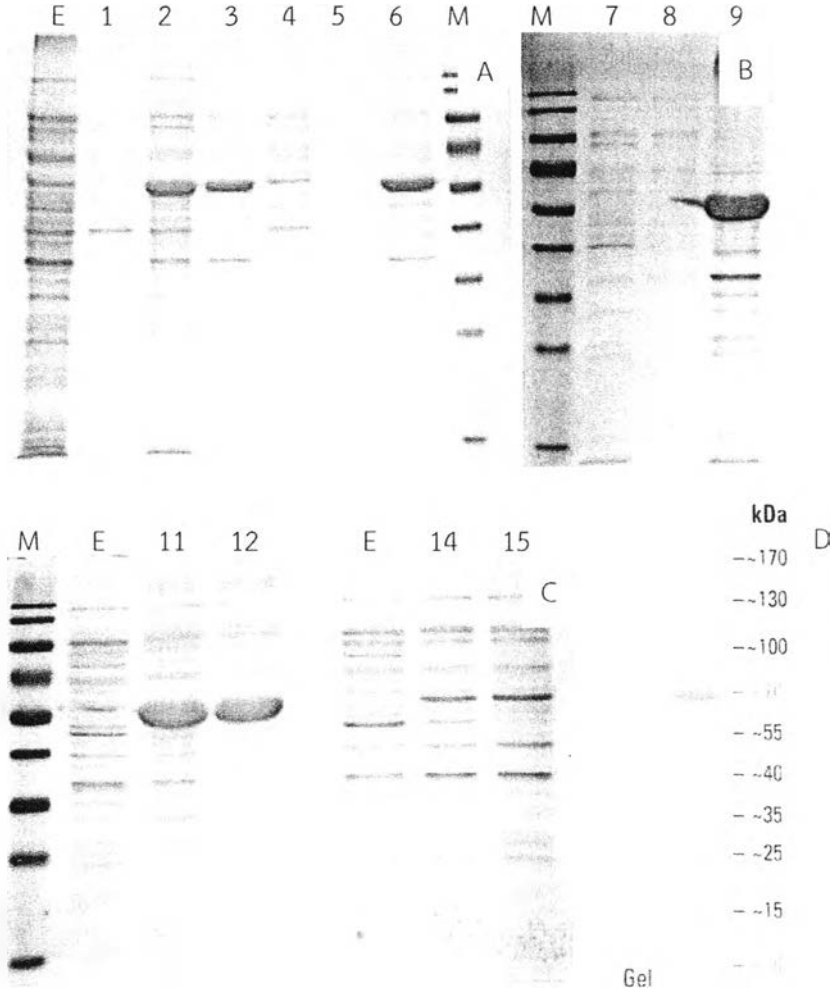

Figure 41 SDS-PAGE of CsGG18H inclusion body using six buffer types. (A) Protein lysate from lysis buffer I and lysis Buffer II (B) protein lysate from lysis buffer III and lysis buffer IV (C) protein lysate from lysis buffer V and lysis buffer VI. (D) Protein marker indicated in lane M. Lane E indicated for empty vector without the recombinant protein.

Lane 1 soluble part of protein lysate in buffer I after sonication **Lane 2** soluble part of protein lysate in buffer I after solubility **Lane 3** pellet part of protein lysate in buffer I after solubility

Lane 4 soluble part of protein lysate in buffer II after sonication **Lane 5** soluble part of protein lysate in buffer II after solubility **Lane 6** pellet part of protein lysate in buffer II after solubility

Lane 7 soluble part of protein lysate in buffer III after sonication **Lane 8** soluble part of protein lysate in buffer III after solubility **Lane 9** pellet part of protein lysate in buffer III after solubility

Lane 10 soluble part of protein lysate in buffer IV after sonication **Lane 11** soluble part of protein lysate in buffer IV after solubility **Lane 12** pellet part of protein lysate in buffer IV after solubility

Lane 14 soluble part of protein lysate in buffer V after sonication **lane 15** soluble part of protein lysate in buffer VI after solubility

5.9 Functional expression of the recombinant enzymes

The expressed products of the two genes CsCPR and CsGG18H as crude enzyme preparations were tested for their activities as follows:

5.9.1 Geranylgeraiol-18-hydroxylase (GG18H) activity

By using geranylgeraniol (GGOH) as the substrate, the CsGG18H preparation was studied for its catalytic activities under various conditions by TLC as the above case of CsG10H. Again, the enzymatic product could be produced only in the reaction containing NADPH and either in the absence of CsCPR (Figure 42) or presence of CsCPR (Figure 42). It should be noted that the intensity of substrate band of GGOH was decreased in the TLC plate with the intensity increase of the product band (Figure 42).

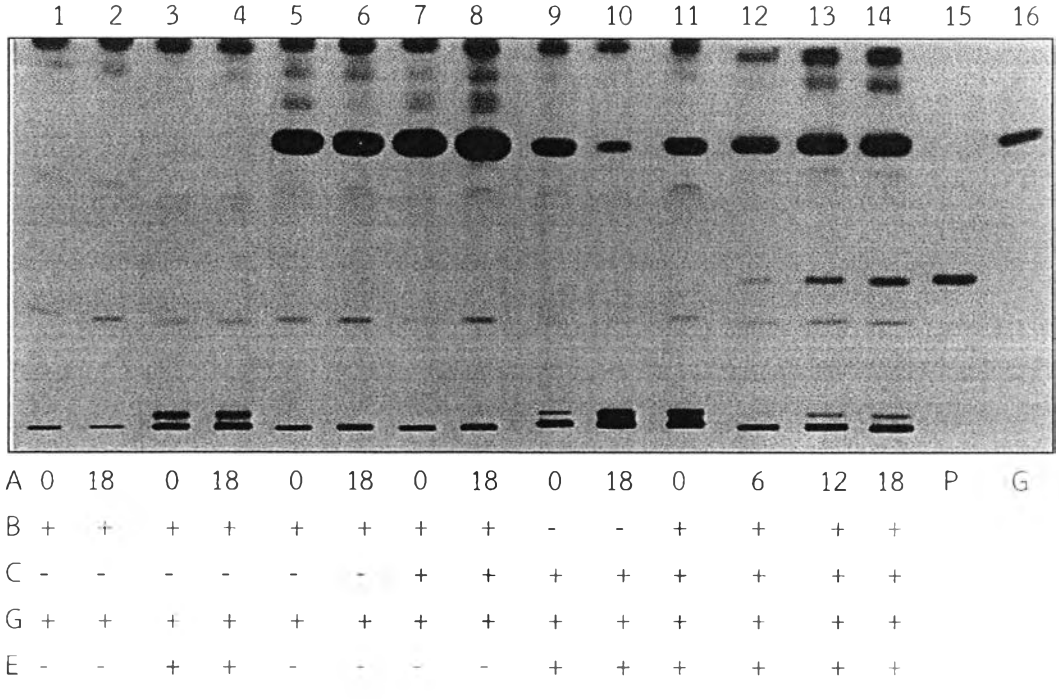

Figure 42 Enzyme activity assays from the recombinant protein of CsGG18H/CsCPR. Crude protein (250 µg) was used in each enzyme assay reaction. The reaction incubated for 18 hr at 37°C. The capital alphabet mean for A: time of incubation; B: CsGG18H; C: CsCPR; D: GGOH, E: NADPH, P: plaunotol standard, G: gernanylgeraniol.

The product band on the TLC were collected and calculated the molecular mass by using the LC-ESI-MS to demonstrated mass measurement. The mass spectrum profile contained $[MS+H]^+$ and $[MS+Na]^+$ ion could be used to confirm the molecular mass of the plaunotol (Figure 43).

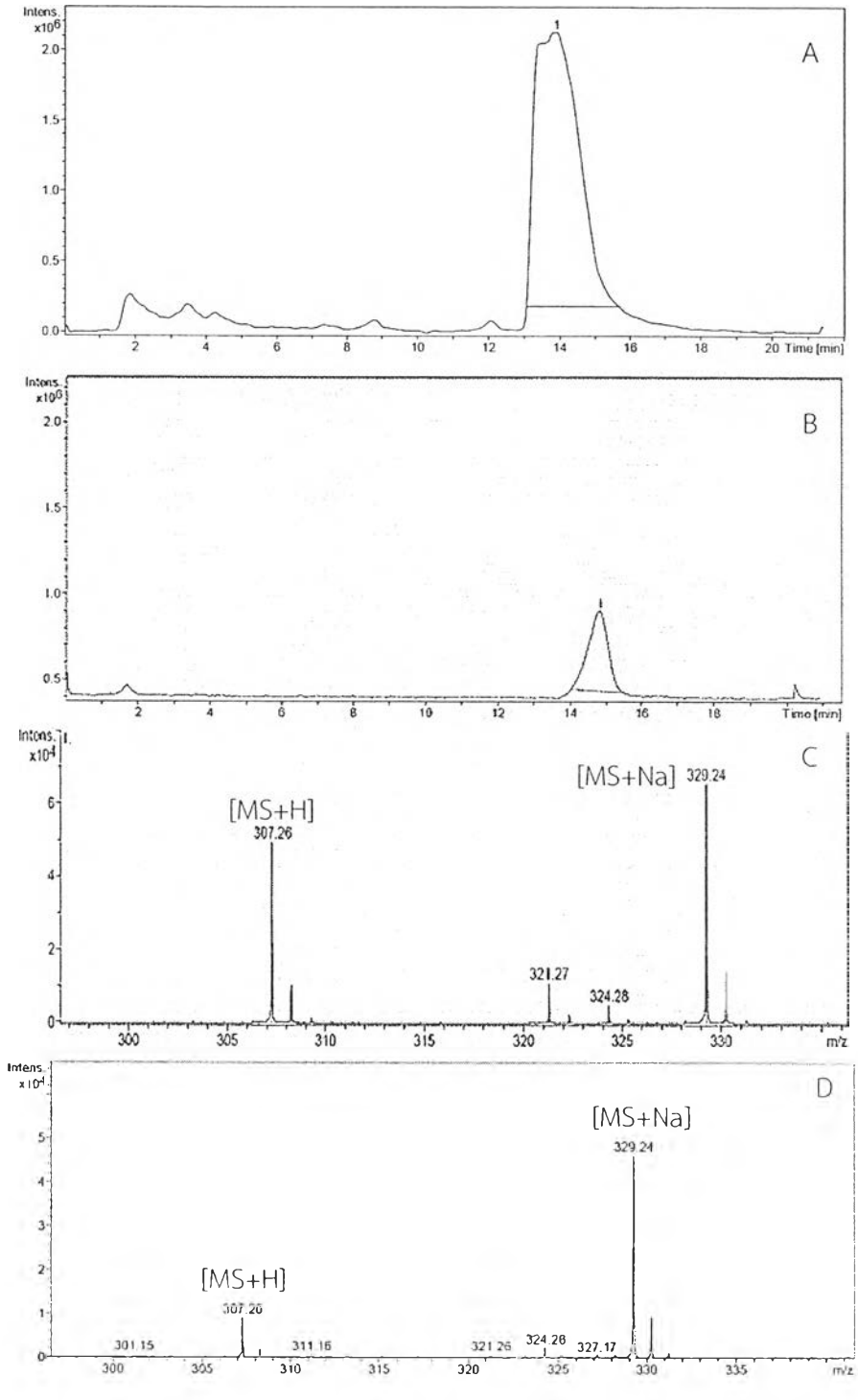

Figure 43 Profile of CsGG18H catalyzed reaction product. (A) The retention time of the plaunotol standard. (B) The retention time of the product of the reaction. (C) LC-ESI-MS chromatogram of the plaunotol standard. (D) LC-ESI-MS chromatogram of the product of the reaction.

5.10 Characterization of the Enzyme

5.10.1 Cytochrome P450, CsGG18H

In order to verify that CsGG18H was cytochrome P450 enzymes, an experiment for P450-carbon monoxide complex formation was performed. This can be done by monitoring the characteristic reduced spectrum of the enzymes after adding and incubating the enzyme with the reducing agent, sodium dithionite. If the absorption spectrum is changed by the shift of the wavelength of the enzyme from 413 nm to 426 nm, this would imply the occurrence of conversion of heme prosthetic group from Fe^{3+} to Fe^{2+}. Moreover, the perturbation of the spectrum at 560 nm implied the charge transfer from the reducing agent to heme center inside enzyme active site. Our results on the monitoring of CO different spectrum after bubbling with CO gas are shown in Figure 44.

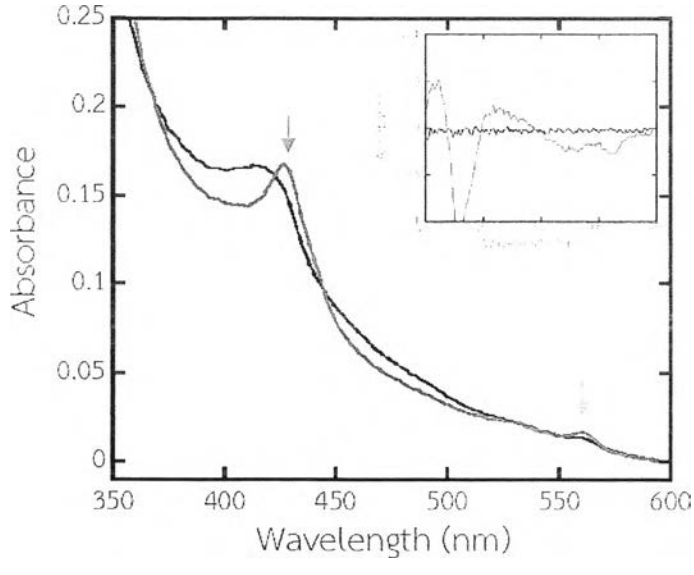

Figure 44 Absorption spectra of cytochrome P450s. CsGG18H in the normal (black) reduced (blue) forms. The red arrow indicates the shift of the absorption from wavelength 413 nm of enzyme in resting state to 426 nm in reduction state. The blue arrow indicates the perturbation of absorption at 560 nm from charge transferring. The insert figures represent CO different spectrum after bubble the reduced enzyme with CO gas and monitoring the absorption change.

5.10.2 Cytochrome P450 Reductase

CPR is a group of flavoprotein dependent enzymes catalyzing the electron transfer from NADPH to FMN-FAD electron acceptor in the enzyme active site and further donates to cytochrome c. The catalytic reaction can be monitored the conversion of cytochrome C from the oxidized to the reduced form with the increased absorption at 550 nm (Butt WD & Keilin D, 1962).

The activity of CsCPR with cytochrome c was tested for the two different co-factor NADH and NADPH follow the protocol described in Section 4.22.4 to analyze the impact on the activity. The CsCPR displayed greater activity with NADPH over NADH as co-factor (Figure 50).

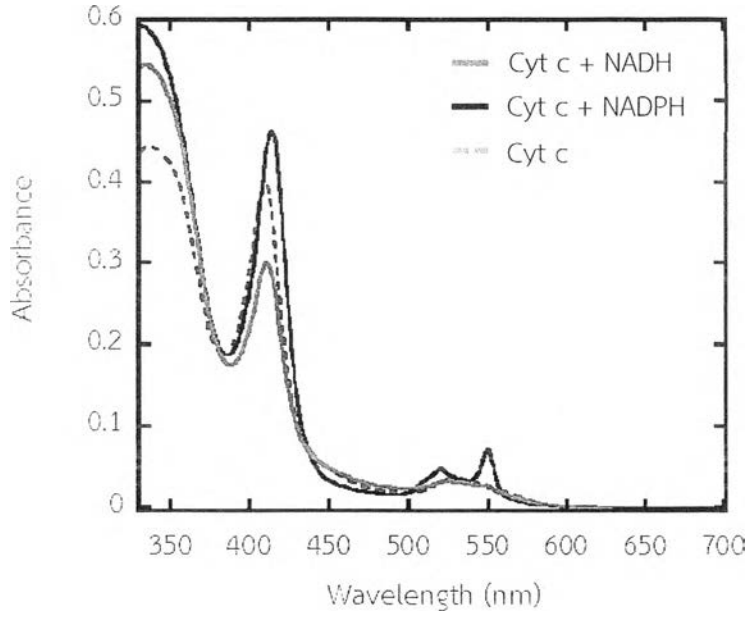

Figure 45 The CsCPR enzymatic activity to NADH and NADPH.

Our results showed that the absorption spectrum was changed from the oxidized to the reduced form of cytochrome c by perturbation at 550 nm in Figure 46.

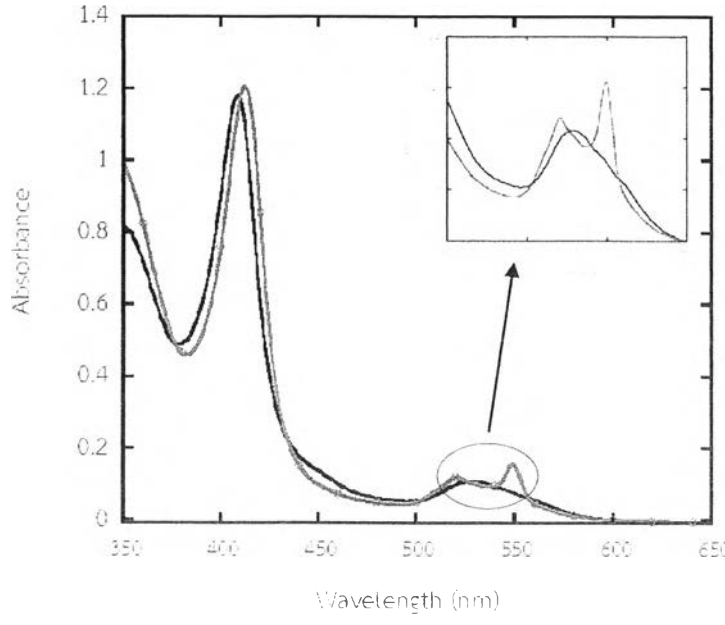

Figure 46 CsCPR catalysis reaction was monitored the perturbation of absorption spectrum at 550 nm. The black solid line indicates cytochrome c in oxidized form and blue solid line indicates the reduced form after reaction is accomplished.

The initial rate of CsCPR was calculated from various cytochrome c and NADPH concentrations under apparent determination by fixed concentration of each substrate. The steady-state kinetic parameters of K_m^{cytC}, K_m^{NADPH} and V_{max} can calculated to be 10.32 + 2.11 μM, 44.77 + 6.047 μM and 0.099 + 0.005 μM min^{-1}, respectively by using non-linear algorithm in KaleidaGraph (Synergy Software) (Figure 47).

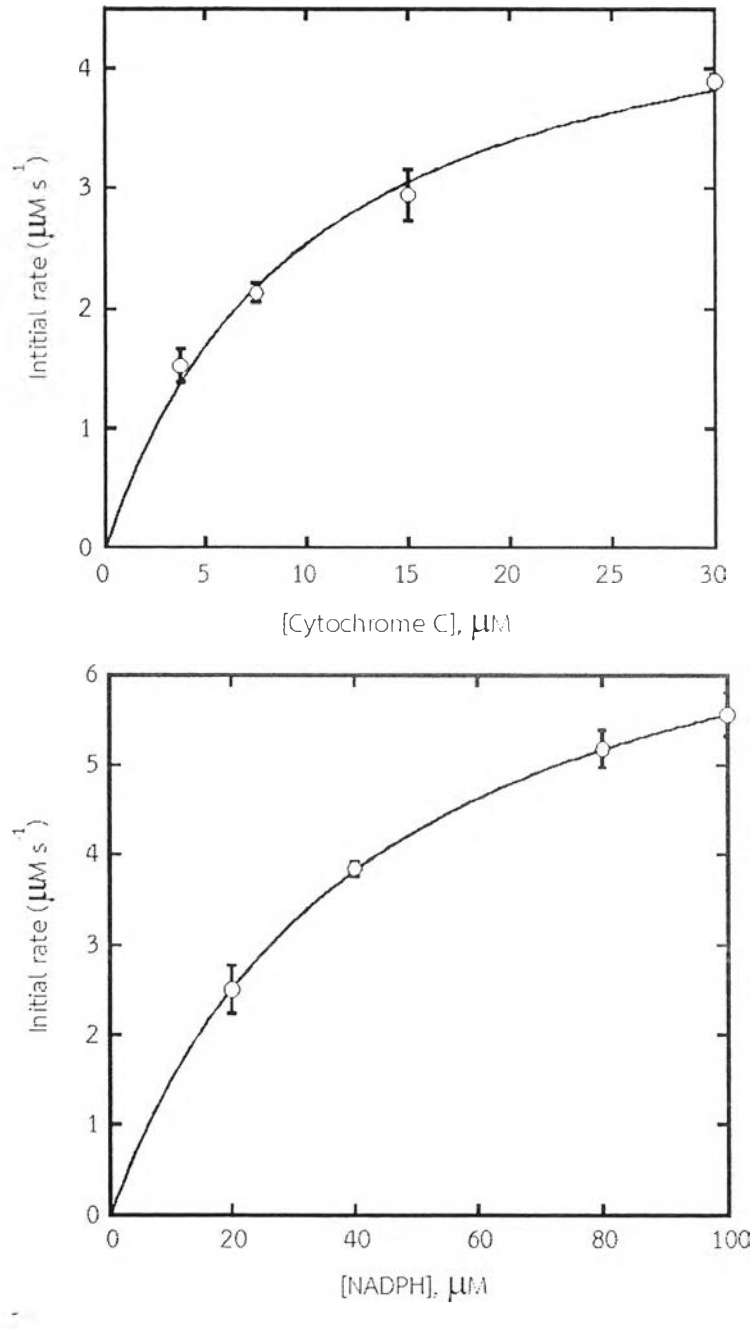

Figure 47 CsCPR steady-state kinetic parameters determination. The initial rate was calculated by vary the concentration of cytochrome c as 3.75-30 μM under fixed NADPH concentration of 120 μM and vary the concentration of NADPH as 20-100 μM under fixed Cytochrome C concentration of 100 μM. CsCPR can determine $K_m^{cyt\ C}$, K_m^{NADPH} and V_{max} to be 10.32 ± 2.11 μM, 44.77 ± 6.047 μM and 0.099 ± 0.005 μM min^{-1}, respectively by using non-linear algorithm in KaleidaGraph (Synergy Software).

5.11 The transcripts of CsGG18H and CsCPR of *C. stelatopilosus*

The transcript profiles of the three enzymes were estimated using real-time PCR. The transcript pattern was found to be related to the plaunotol content. As shown in Figure 48 the plaunotol was accumulated in high content in leaf 5 estimated by dry weight (Figure 48A). The plaunotol contents were differed between the part of the plant that shown in Figure 48B. The plaunotol content highest in leaf and seem not presented in twig (Figure 48B).

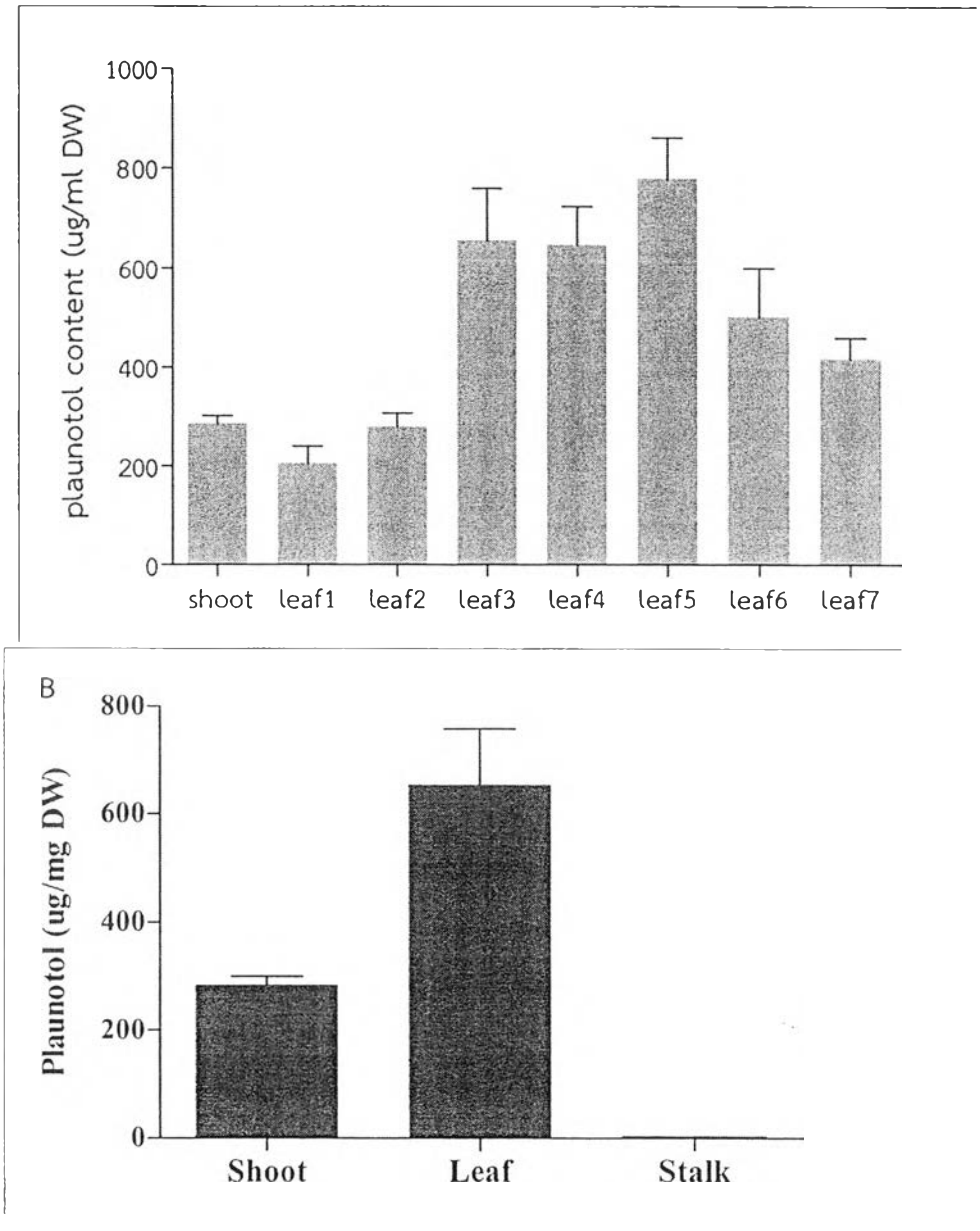

Figure 48 Plaunotol content. (A) Plauntotol contents according to the leaf development containing the shoot and the first leaf to the seventh leaf away from shoot. (B) Plaunotol content found in shoot, the third leaf and stalk.

The *CsGG18H*, and *CsCPR* were presented in every shoot and other 5 leaf position in development stages (Figure 49A). However, there is the different in expression level compared between each shoot, leaf and twig (Figure 49B). The results indicate that *CsCPR* had a maximum transcript is also detected in 1st position leaf and the others were decreased and fluctuated (Figure 49A). Transcripts of the *CsGG18H* seem highest in 3rd position leaf and still constantly trough the 5th leaf.

The plant parts were the shoot, leaf and stalk, and the genes selected were DXS and MEPS, the first two genes of the MEP pathway, *GGPPS* and *GGPPP*, the first two genes of the plaunotol pathway, and *CsGG18H* and CsCPR, the last two genes of the pathway. All five genes were fully expressed in the leaf, whereas there was limited expression of *GGPPS* and relatively low levels of CsGG18H in the shoot. *DXS*, *MEPS* and *CsGG18H* were rarely expressed. These transcription profiles were consistent with the plaunotol content profile in each of plant part.

The pattern of the expression of *CsCYP* and *CsGG18H* had the same trends in the increasing of transcripts found in other gene involving in plaunotol biosynthesis. This evident are supported the plaunotol synthesis (the plaunotol contents accumulated in, Figure 48) related to the expression level of *CsCPR* and *GG18H* with the impact of plaunotol biosynthesis.

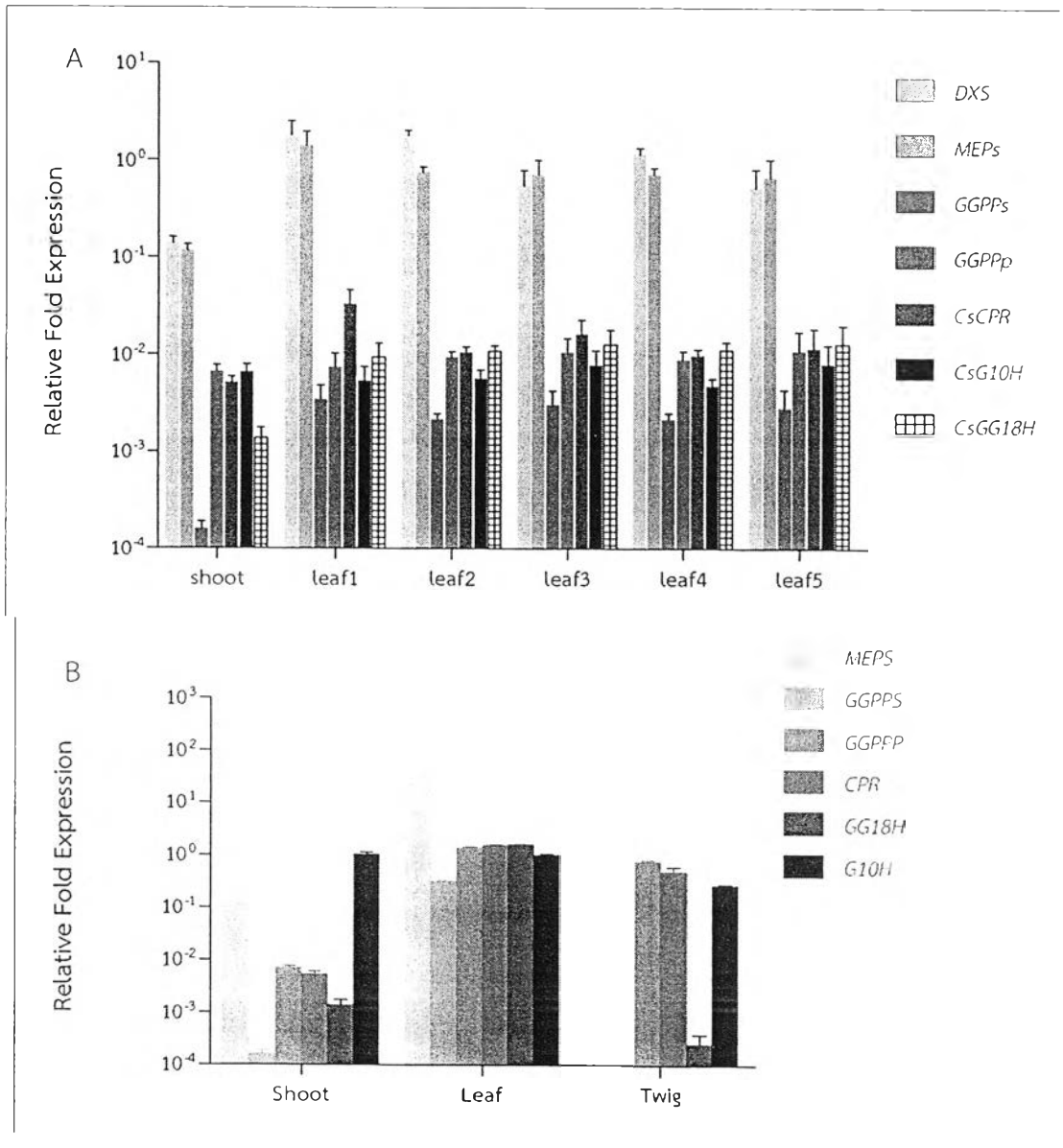

Figure 49 The relative real-time PCR. (A) Seven genes involving in the terpenoid pathway expressed throughout the leaf development. (B) Seven genes involving in the terpenoid pathway expressed throughout the shoot, leaf and stalk in *C. stellatopilosus* were monitored.